Discrimination of Axial and Central Stereogenic Elements in Chiral Bis(oxazolines) Based on Atropisomeric 3,3′-Bithiophene Scaffolds Through Chiroptical Spectroscopies

SARA GABRIELI,[1] GIUSEPPE MAZZEO,[2] GIOVANNA LONGHI,[2,3] SERGIO ABBATE[2,3]* AND TIZIANA BENINCORI[1]**

[1]*Dipartimento di Scienza ed Alta Tecnologia-DISAT, Università dell'Insubria, Como, Italy*
[2]*Dipartimento di Medicina Molecolare e Traslazionale - DMMT, Università di Brescia, Brescia, Italy*
[3]*CNISM Consorzio Nazionale Interuniversitario per le Scienze Fisiche della Materia, Roma, Italy*

ABSTRACT Two diastereoisomeric pairs of bis-oxazolines, provided with a stereogenic center at carbon 4 and based on the 3,3′-bithiophene atropisomeric scaffold, were synthesized and structurally characterized. They differ in the substituents at positions 2 and 5 of the thiophene rings, which are functionalized with methyl (1) or phenyl (2) groups, respectively. In vibrational circular dichroism (VCD) spectra, recorded in CCl_4 solutions, it is possible to distinctly recognize the characteristic features of axial and central stereogenic elements. In tandem with Density Functional Theory (DFT) calculations, the absolute configuration (AC) of the diastereoisomers was safely established. In this case, VCD was shown to be superior to ECD (electronic circular dichroism) in the assignment of AC. The normal modes, evaluated from DFT calculations, show that the VCD signals in correspondence with the stereogenic axis of the bithiophene unit are different for 1 and 2. The VCD spectra of a molecular analog of 1, the (S)-2,2′,5,5′-tetramethyl-4,4′-bis-(diphenylphosphino)-3,3′-bithiophene oxide (3), characterized by the same 3,3′-bithiophene scaffold, but devoid of stereogenic centers, exhibits signals similar to those observed in the case of diastereoisomer (aS,R,R)-1a, associated with almost identical normal modes. *Chirality 28:686–695, 2016.*

KEY WORDS: bithiophene; atropisomers; electronic circular dichroism (ECD); vibrational circular dichroism (VCD); Density Functional Theory calculations (DFT)

The key to success of an asymmetric catalytic process is related to the efficiency of the catalyst and it is well documented that each reaction requires a specific mediator to attain high enantioselection levels and fast reaction rates. One strategy in this direction is organometallic catalysis, in which the chiral catalysts are organometallic complexes of a transition metal, which becomes the reaction center. The metal is complexed with a chiral ligand, which enables it to perform the enantiofacial recognition process on the prostereogenic substrate. A different approach is offered by organic catalysis, where organic molecules perform the same role of organometallic complex without requiring metal complexation.

In the first approach, thousands of chiral ligands have been prepared so far, endowed with different stereogenic elements, although a relatively small number of them emerge for applicability, scope, and synthetic accessibility.

In the past, we were involved in homogeneous stereoselective catalysis identifying an atropisomeric biheteroaromatic scaffold as the key structural element for designing a versatile class of chiral promoters.[1]

In particular, we investigated deeply a very successful family of biheteroaromatic diphosphines as ligands for transition metals in the hydrogenation of prostereogenic carbon–carbon and carbon–oxygen double bonds,[2–4] in the Diels-Alder cycloaddition of cyclopentadiene and *N*-2-alkenoyl-1,3-oxazolidine-2-ones[5] and in some inter-[6] and intramolecular Heck reactions.[7] The results obtained from these studies pointed out that the 3,3′-bithiophene atropisomeric scaffold was efficient both in kinetically promoting the reactions and in enhancing the stereoselectivity levels.[8]

We then focused our attention on a different class of ligands and investigated the role played by either the electronic or the steric features of bis(oxazoline)ligands, carrying flexible and atropisomeric 3,3′-bithiophene backbones, in the Cu(I)-catalyzed cyclopropanation of styrene effected with ethyl diazoacetate.[9] This investigation suggested that steric factors and catalyst geometrical features are preeminent over the electronic properties of the chiral ligands.

This article reports an effort to widen the family of the chiral bis(oxazoline)ligands based on the atropisomeric 3,3′-bithiophene skeleton. For this purpose, we synthesized and structurally characterized the two pairs of diastereoisomeric bis(oxazolines) **1** and **2,** mainly differing in the steric properties of the substituents on the atropisomeric scaffold (Scheme 1).

It is imperative to define the absolute configuration (AC) of the new compounds. As the primary 3D property responsible for stereoselection efficiency of the catalyst, we resorted to chiroptical methods, especially electronic circular dichroism (ECD) and vibrational circular dichroism (VCD)[10–17] as fast and reliable techniques. In fact, they represent reliable and ef-

*Correspondence to: Sergio Abbate, Dipartimento di Medicina Molecolare e Traslazionale, DMMT, Università di Brescia, Viale Europa 11, 25123 Brescia, Italy.
Tiziana Benincori, Dipartimento di Scienze ed Alta Tecnologia-DISAT Università dell'Insubria, Via Valleggio 11, 22100 Como, Italy. E-mail: sergio.abbate@unibs
Received for publication 16 June 2016; Accepted 1 August 2016
DOI: 10.1002/chir.22633
Published online in Wiley Online Library (wileyonlinelibrary.com).

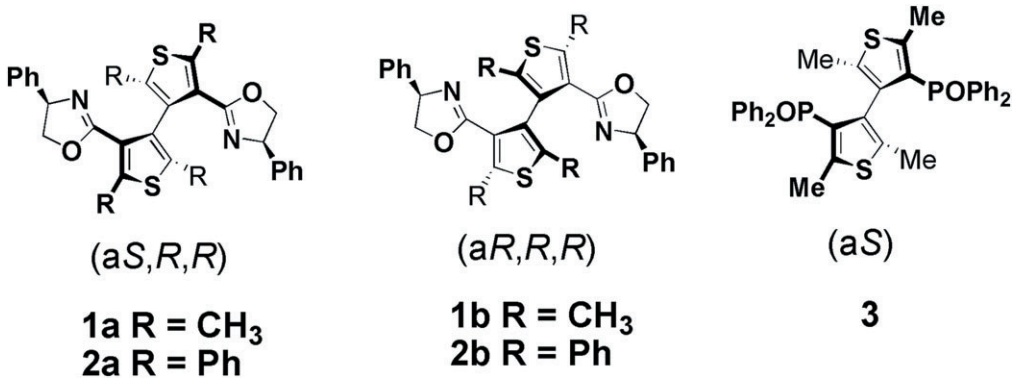

Scheme 1. Structures of compounds **1**-**3** studied in the present work.

ficient alternatives to X-ray diffraction analysis, which is the never-failing experimental method for the definition of molecular shape, including conformation and configuration, but not always applicable, since it works on single-crystal samples only.

We expected that VCD could be a particularly sensitive tool to discriminate the effects of central and axial stereogenicity in **1** and **2**, since ECD is mostly sensitive to the stereogenic units constituted by inherently dissymmetric chromophores, like cyclophanes and biaryls. Accordingly, we already successfully employed this technique to investigate the chiroptical signatures of planar and central stereogenic elements in [2]paracyclo[2](5,8)-quinolinophane derivatives.[18]

We should like to point out that the co-presence of axial and central stereogenic elements (centers) has been monitored by VCD only recently,[19,20] and even axial stereogenicity *per se* has seldom been treated by VCD, with respect to the large number of studies devoted to central stereogenicity.[21,22] This fact may result in an added value of the present study. To establish whether the findings for **1a** and **1b** would have a general character, we also considered the (*S*)-2,2′,5,5′-tetramethyl-4,4′-bis-(diphenylphosphino)-3,3′-bithiophene oxide (**3**),[8] which shares the same central stereogenic motif as **1a**, but it is devoid of the additional stereogenic centers of the oxazoline ring (Scheme 1).

MATERIALS AND METHODS

All VCD/IR spectra were taken with a Jasco (Tokyo, Japan) FVS6000 FTIR spectrometer equipped with a VCD module, comprised of a wire-grid linear polarizer, a ZnSe Photo Elastic Modulator (PEM) to produce 50 kHz modulated circularly polarized radiation over a rather wide range (from 3000 to 800 cm^{-1}), and a liquid N_2-cooled MCT detector. The spectra were recorded in CCl_4 solutions in the concentration range of 0.1–0.2 M, in 200 μm BaF_2 cells. A total of 2000 scans were taken for each spectra and subtraction of VA and VCD spectra of the solvent were performed. ECD/UV spectra were taken with a Jasco 815SE spectrometer and 0.1 mm quartz cells were employed; with acetonitrile solutions at a concentration of 0.0015 M. For thin-layer chromatography (TLC) analysis, precoated TLC sheets ALUGRAM Xtra SIL G/UV254 were used. Column chromatography was performed on 230–400 mesh Sigma-Aldrich (St. Louis, MO) silica gel. Melting point determinations were performed by using a Büchi B-540 instrument. ^{1}H-NMR and ^{13}C-NMR were measured on a Bruker (Billerica, MA) FT 300 or Bruker AMX 300. Chemical shifts (δ) are expressed in parts per million (ppm) and coupling constants are reported as Hertz (Hz). Splitting patterns are indicated as follows: s = singlet, d = doublet, t = triplet, q = quartet, m = multiplet, br s = broad singlet, br d = broad doublet. Mass analyses were performed using a VG 7070 EQ-HF instrument.

Computational Details

Prior to DFT calculations, a molecular mechanics (MM) search of conformers within 5 kcal/mol was performed. The conformers thus found were fed to the DFT module of Gaussian09,[23] which was run at the B3LYP/TZVP level of theory; besides better definition of the conformers found at the MM level, with appropriate statistical weights, calculation of dipole and rotational strengths through the field-response approach[24] was possible. From calculated frequencies, dipole and rotational strengths, VA and VCD spectra were generated by assigning an 8 cm^{-1} bandwidth Lorentzian bandshape to each vibrational transition with a program resident on the Jasco VCD software package. A scaling factor of 0.98 was applied to all calculated vibrational transitions. Dipole and rotational strengths (for the first 30 excited states) in the UV range were calculated by means of TD-DFT at the CAM-B3LYP/TZVP level of theory. Theoretical ECD spectra were obtained from calculated excitation energies and rotational strengths (as averages weighed on Boltzmann conformers relative populations) as sum of Gaussian functions centered at the wavelength of each transition with a width of the band at half-height of 0.2 eV using SpecDis v1.64.[25] Simulation of VCD spectra was carried out in vacuo, since the solvent employed in experiments was apolar (CCl_4); simulation of ECD spectra was carried out in the PCM approximation, since CH_3CN was employed as a solvent.

Synthesis of (bis)oxazolines 1 and 2

*Synthesis of 4,4′-dibromo-2,2′,5,5′-tetraphenyl-3,3′-bithiophene (**10**):* hexabromo-3,3′-bithiophene.[26] (0.5 g, 0.78 mmol), phenyl boronic acid (0.62 g, 5.1 mmol), and K_2CO_3 (0.65 g, 4.7 mmol) were dissolved in dry toluene (20 mL) under N_2 atmosphere; after 10 min stirring, tetrakis (triphenylphosphine)palladium(0) (Pd(tetrakis)) (0.027 g, 0.023 mmol) was added and the mixture was heated at reflux for 24 h. The solvent was removed under reduced pressure and the crude was dissolved in dichloromethane (20 mL) and washed with water (20 mL); the organic layer was dried and concentrated in vacuo. Flash chromatography (*n*-hexane/CH_2Cl_2 9:1) led to compound **10** as a yellow solid, which was triturated in *n*-hexane to give **10** as a white solid, 60% yield. (Scheme 2).

^{1}H NMR (300 MHz, $CDCl_3$, *δ):* 7.80–7.78 (d, 4H, *J* = 6 Hz), 7.49–7.47 (t, 2H, *J* = 6 Hz), 7.42–7.40 (d, 4H, *J* = 6 Hz), 7.23–7.09 (m, 10H); ^{13}C NMR (75.4 MHz, $CDCl_3$, δ): 141.9 (C), 137.1 (C), 133.6 (C), 133.4 (C), 133.1 (C), 129.1 (CH), 128.6 (CH), 128.5 (CH), 128.4 (CH), 127.9 (CH), 127.8 (CH), 11.7 (C); mp: 127.5 °C; EIMS (m/z) 629 [M^+].

*Synthesis of 2,2′,5,5′-tetraphenyl-3,3′-bithiophene-4,4′-dicarboxylic acids **7**:* *n*-BuLi (1.5 M solution in hexane, 24 mL) was slowly added to a solution of the dibromo derivative **10** (8 mmol) in dry diethyl ether (30 mL), at −70 °C under argon atmosphere; after 1 h stirring, dry $CO_{2(g)}$ was bubbled into the reaction mixture at −50 °C, then the mixture was stirred at room temperature overnight. The solvent was removed under reduced pressure, then water (30 mL) and CH_2Cl_2 (3 mL) were added to the residue. The aqueous layer was separated and the organic one was extracted with a 10% K_2CO_3 solution (30 mL). The combined aqueous layers were acidified with a conc. HCl solution (30 mL). The precipitated

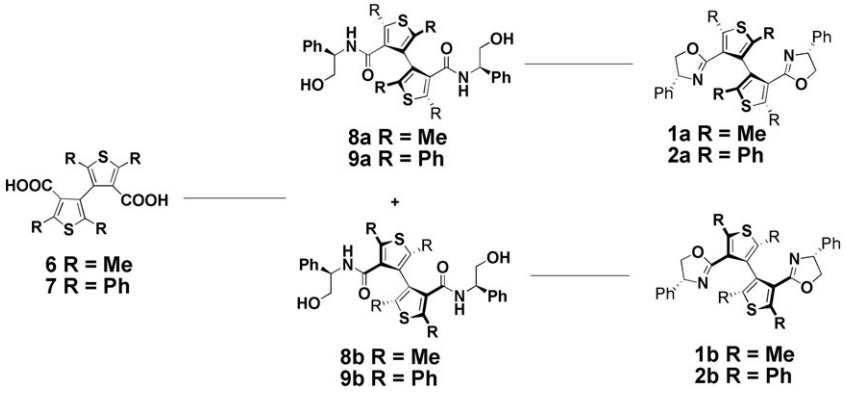

Scheme 2. General strategy for the synthesis of bis(oxazolines) **1a,b** and **2a,b.**

product was collected and dried to give the title product in good purity as a pale yellow solid, 62% yield. ^{1}H NMR (300 MHz ,$CDCl_3$, δ): 7.56–7.53 (m, 4H), 7.41–7.39 (m, 6H), 7.15–7.05 (m, 6H), 6.69–6.67 (m, 4H); ^{13}C NMR (75.4 MHz, $CDCl_3$, δ): 207.0 (C), 168.8 (C), 142.2 (C), 133.3 (C), 133.1 (C), , 132.4 (C), 129.4 (CH), 128.7 (CH), 128.6 (CH), 128.3 (CH), 128.1 (CH), 127.4 (CH); mp > 240 °C; EIMS (m/z) 558 [M^+] (Scheme 3).

*Synthesis of (S/R)-N,N´-bis[(R)-2-hydroxy-1-phenylethyl]-2,2´,5,5´-tetramethyl-3,3´-bithiophene-4,4´-dicarboxamide (**8a** and **8b**)* (Scheme 4): $SOCl_2$ (4 mL) was slowly added to a solution of dicarboxylic acid **6**[9] (1 g, 3.23 mmol) in dry CH_2Cl_2 (15 mL); the reaction mixture was stirred at reflux for 5 h, then the excess of thionyl chloride was removed under reduced pressure. The solution of the acid dichloride (3.23 mmol) in dry CH_2Cl_2 (6 mL) was dropped, under nitrogen, at 0 °C into a stirred solution of TEA (0.9 mL, 6.46 mmol) and (*R*)-phenylglycinol (0.89 g,6.46 mmol) in dry CH_2Cl_2 (6 mL). The reaction mixture was stirred at room temperature overnight, then washed with 1 N HCl solution (10 mL) and then with water (10 mL). The organic layer was separated, dried over Na_2SO_4, and the solvent removed under reduced pressure. The crude residue was purified by flash chromatography (AcOEt/hexane 7:3) and the two diastereomeric diamides were obtained in a high purity state. The first fractions eluted were evaporated to dryness to give **8a** as brownish solid, 29% yield. ^{1}H NMR (300 MHz ,$CDCl_3$, δ): 7.30–7.28 (m, 6H), 7.09–7.07 (m, 4H), 6.75 (br d, 2NH), 5.07–5.02 (m, 2H), 3.69 (t, 4H, J = 5.1 Hz), 2.51 (s, 6H), 2.50 (br s, 2OH), 2.17 (s, 6H); ^{13}C NMR (75.4 MHz, $CDCl_3$, δ): 166.3 (C), 139.1 (C), 137.9 (C), 134.7 (C), 134.5 (C), 130.9 (C), 128.5 (CH), 127.5 (CH), 126.7 (CH), 65.6 (CH_2), 55.6 (CH), 14.1 (CH_3), 13.2 (CH_3); mp 175–176 °C; EIMS (m/z) 548 [M^+].

The last fractions eluted were evaporated to dryness to give **8b** as brown solid, 29% yield. ^{1}H NMR (300 MHz ,$CDCl_3$, δ): 7.29–7.25 (m, 6H), 7.06–7.03 (m, 4H), 6.65 (br s, 1H), 5.06–5.00 (m, 2H), 3.83 (dd, 2H, *J* = 11.7, *J* = 3.3), 3.60 (dd, 2H, *J* = 11.7, *J* = 5.7), 3.32 (br s, 2NH), 2.61 (s, 6H), 2.14 (s, 6H) ; ^{13}C NMR (75.4 MHz, $CDCl_3$, δ): 165.6 (C), 140.7 (C), 139.0 (C), 134.4 (C), 133.0 (C), 130.8 (C), 128.5 (CH), 127.5 (CH), 126.6 (CH), 65.8 (CH_2), 56.0 (CH), 14.8 (CH_3), 13.2 (CH_3); mp 104–106 °C; EIMS (m/z) 548 [M^+].

*Synthesis of (S,R)-N,N´-bis[(R)-2-hydroxy-1-phenylethyl]-2,2´,5,5´-tetraphenyl-3,3´-bithiophene-4,4´- dicarboxamide **9a** and **9b*** (Scheme 5): Dicarboxylic acid **7** (0.38 g 0.69 mmol) was dissolved in dry CH_2Cl_2 (8 mL) and the solution stirred under N_2 atmosphere; HATU (0.627 g, 1.65 mmol), HOAt (0.225 g, 1.65 mmol), and DIPEA (0.9 mL, 5.51 mmol) were added at 0 °C. After 30 min, (*R*)-phenylglycinol (0.19 g, 1.38 mmol) was added and the reaction mixture stirred overnight. The reaction mixture was washed with 1 N HCl solution (10 mL) and the organic layer dried and concentrated under reduced pressure. The two diastereomeric

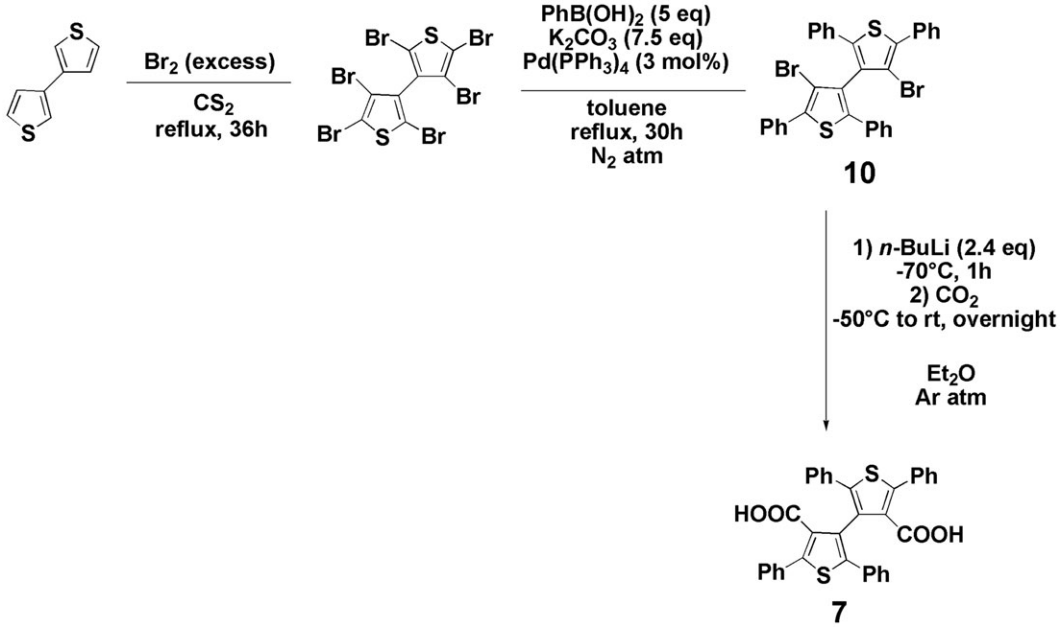

Scheme 3. Synthesis of dicarboxylic acid **7.**

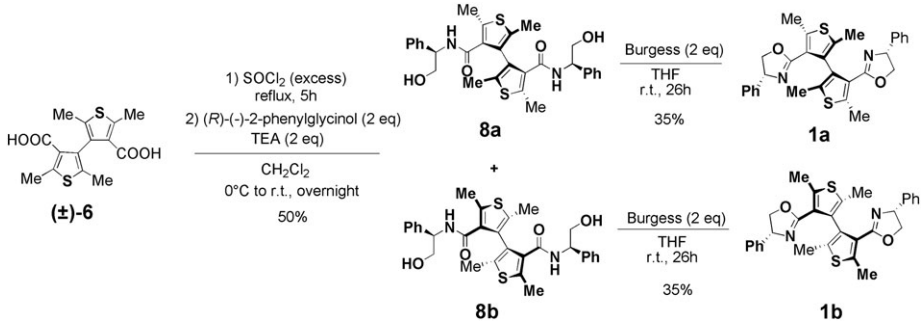

Scheme 4. Synthesis of (*aS*)- and (*aR*)-2,2′,5,5′-tetramethyl-4,4′-bis[(*R*)-4,5-dihydro-4- phenyloxazol-2-yl]-3,3-bithiophene **1a** and **1b.**

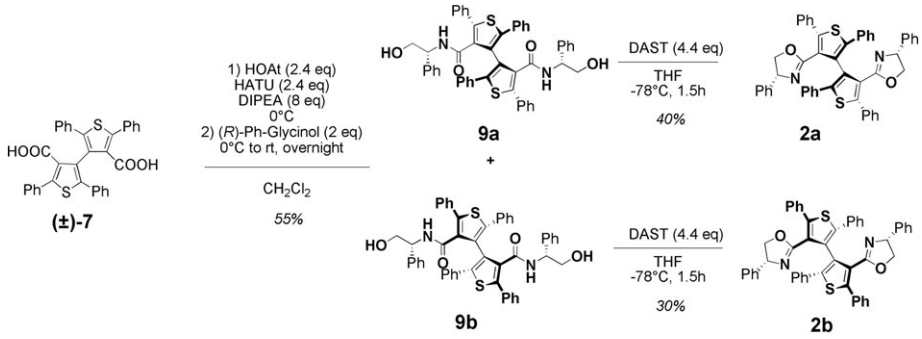

Scheme 5. Synthesis of (*aS*)- and (*aR*)-2,2′,5,5′-tetraphenyl-4,4′-bis[(*R*)-4,5-dihydro-4- phenyloxazol-2-yl]-3,3-bithiophene **2a** and **2b.**

amides were separated by flash chromatography (CH_2Cl_2/AcOEt 9:1) and the first fractions eluted were evaporated to dryness to give **9a** as a pale yellow solid, 28% yield. ^{1}H NMR (300 MHz ,$CDCl_3$, δ): 7.56–7.53 (m, 4H), 7.35–7.30 (m, 10H), 7.25–7.22 (m, 6H), 7.20–7.18 (m, 6H), 7.08 (br d, 2NH), 7.01–6.98 (m, 4H), 5.03 (dt, 2H, *J* = 10.5 Hz, *J* = 5.4 Hz), 3.61 (d, 4H, *J* = 5.4 Hz), 2.50 (br s, 2OH); ^{13}C NMR (75.4 MHz ,$CDCl_3$, δ): 166.7 (C), 142.0 (C), 141.3 (C), 138.5 (C), 136.1 (C), 133.1 (C), 132.6 (C), 130.7 (C), 129.0 (CH), 128.8 (CH), 128.5 (CH), 128.1 (CH), 127.7 (CH),127.0 (CH), 65.7 (CH_2), 56.1 (CH); mp 195–198 °C; EIMS (m/z) 796 [M^+].

The last fractions eluted were evaporated to dryness to give **9b** as a pale yellow solid, 28% yield. ^{1}H NMR (300 MHz ,$CDCl_3$, δ):8.01 (br d, 2NH), 7.38–7.35 (m, 4H), 7.27–7.24 (m, 8H), 7.18–7.15 (m, 10H), 7.08–7.06 (m, 4H), 6.88 (d, 4H), 6.50 (br s, 2OH), 4.92 (q, 2H), 3.65 (d, 4H, *J* = 5.6 Hz).; ^{13}C NMR (75.4 MHz ,$CDCl_3$, δ): 167.3 (C), 144.1 (C), 138.4 (C), 133.1 (C), 132.3 (C), 130.5 (C), 129.9 (CH), 129.6 (CH), 129.2 (CH), 129.0 (CH), 128.3 (CH),128.1 (CH), 127.1 (CH), 66.1 (CH_2), 57.3 (CH); mp 127–131 °C; EIMS (m/z) 796 [M^+].

Synthesis of (S)-2,2′,5,5′-tetramethyl-4,4′-bis[(R)-4,5-dihydro-4-phenyloxazol-2-yl]-3,3-bithiophene **1a** (Scheme 4): The Burgess reagent (methyl *N*-[[(triethylammonium)sulphonyl]carbamate] (0.313 g,1.31 mmol,) was added to a solution of the dicarboxamide **8a** (0.36 g, 0.656 mmol) in dry THF (4 mL). The reaction mixture was stirred for 26 hours, then the solvent was removed under reduced pressure and the crude was chromatographed under pressure (AcOEt/*n*-hexane 4:6) to give **1a** as a dense colorless oil, 35% yield. ^{1}H NMR (300 MHz ,$CDCl_3$, δ): 7.33–7.25 (m, 6H), 7.18–7.15 (m, 4H), 5.24 (dd, 2H, J = 10.2 Hz, *J* = 8.1 Hz), 4.50 (dd, 2H, *J* = 10.2 Hz, *J* = 8.4 Hz), 3.92 (t, 2H, *J* = 8.1 Hz), 2.69 (s, 6H), 2.25 (s, 6H). ^{13}C NMR (75.4 MHz, $CDCl_3$, δ): 162.1 (C), 142.9 (C),.139.4 (C), 133.1 (C), 128.5 (CH), 127.3 (CH), 126.6 (CH), 126.2 (C), 74.1 (CH_2), 69.9 (CH), 15.0 (CH_3),13.7 (CH_3); EIMS (m/z) 512 [M^+].

Synthesis of (R)-2,2′,5,5′-tetramethyl-4,4′-bis[(R)-4,5-dihydro-4-phenyloxazol-2-yl]-3,3-bithiophene **1b** (Scheme 4): The Burgess reagent (0.313 g,1.31 mmol,) was added to a solution of the dicarboxamide **8b** (0.36 g, 0.656 mmol) in dry THF (4 mL). The reaction mixture was stirred for 26 h, then the solvent was removed under reduced pressure and the crude was chromatographed under pressure (AcOEt/*n*-hexane 4:6) to give **1b** as a dense colorless oil, 35% yield. ^{1}H NMR (300 MHz ,$CDCl_3$, δ): 7.29–7.18 (m, 10H), 5.25 (dd, 2H, *J* = 10.2 Hz, *J* = 8.1 Hz), 4.46 (dd, 2H, *J* = 10.2 Hz, *J* = 8.4 Hz), 3.96 (t, 2H, *J* = 8.4 Hz), 2.71 (s, 6H), 2.18 (s, 6H). ^{13}C NMR (75.4 MHz, $CDCl_3$, δ): 162.2 (C), 143.1 (C),.139.6 (C), 133.4 (C), 128.3 (CH), 127.3 (CH), 126.8 (CH), 126.6 (C), 74.2 (CH_2), 70.1 (CH), 15.2 (CH_3), 13.9 (CH_3); EIMS (m/z) 512 [M^+].

Synthesis of (S)-2,2′,5,5′-tetraphenyl-4,4′-bis[(R)-4,5-dihydro-4-phenyloxazol-2-yl]-3,3-bithiophene ***2a*** (Scheme 5): Pure diamide **9a** (0.64 g, 0.8 mmol) was dissolved in THF (6.5 mL) and the solution cooled at −78 °C, then DAST (0.5 mL, 3.52 mmol) was added dropwise and the reaction mixture stirred at the same temperature for 90 min. The mixture was filtered and the solvent evaporated under reduced pressure. The residue was purified by flash chromatography (AcOEt/*n*-hexane 3:7) to give **2a** as a pasty oil, 40% yield.^{1}H NMR (300 MHz, MeOD, δ): 7.64–7.57 (m, 4H), 7.45–7.38 (m, 6H), 7.15–6.97 (m, 20H), 5.22 (t, 2H, *J* = 9.9 Hz), 4.62 (t, 2H, *J* = 9.9 Hz), 4.02 (t, 2H, *J* = 8.7 Hz); ^{13}C NMR (75.4 MHz, $CDCl_3$, δ): 161.7 (C), 143.4 (C), 142.4 (C), 141.8 (C), 133.4 (C), 132.9 (C), 129.1 (CH), 128.7 (CH), 128.4 (CH), 128.3 (CH), 127.9 (CH), 127.3 (CH), 127.03 (CH), 126.7 (CH), 74.5 (CH_2), 70.1 (CH); EIMS (m/z) 760 [M^+].

Synthesis of (R)-2,2′,5,5′-tetraphenyl-4,4′-bis[(R)-4,5-dihydro-4-phenyloxazol-2-yl]-3,3-bithiophene ***2b*** (Scheme 5): Pure diamide **9b** (0.64 g, 0.8 mmol) was dissolved in THF (6.5 mL) and the solution cooled at −78 °C, then DAST (0.5 mL, 3.52 mmol) was added dropwise and the reaction mixture stirred at the same temperature for 90 min. The mixture was filtered and the solvent evaporated under reduced pressure. The residue was purified by flash chromatography (AcOEt/*n*-hexane 3:7) to give **2b** as a pasty oil, 30% yield.^{1}H NMR (300 MHz, $CDCl_3$, δ): 7.73–7.41 (m, 4H), 7.44–7.42 (m, 6H), 7.19–7.11 (m, 12H), 7.05–6.99 (m, 8H), 5.32 (t, 2H, *J* = 9.3 Hz), 4.59 (dd, 2H, *J* = 10.2 Hz, *J* = 8.1 Hz), 4.05 (t, 2H, *J* = 8.4 Hz); ^{13}C NMR (75.4 MHz, $CDCl_3$, δ): 161.1 (C), 143.8 (C), 142.4 (C), 141.1 (C), 128.8 (C), 128.5 (C), 129.3 (CH), 128.8 (CH), 128.6 (CH), 128.4 (CH), 128.2 (CH), 127.5 (CH), 127.02 (CH), 126.6 (CH), 125.8 (CH), 74.1 (CH_2), 70.0 (CH); EIMS (m/z) 760 [M^+].

RESULTS AND DISCUSSION

Synthesis of Bis(oxazolines) 1 and 2

The synthesis of all the bis(oxazolines) followed the usual strategy, starting from the dicarboxylic acids **6** and **7**, which were converted into the diamides **8a**,**b** and **9a**,**b** by reaction with (*R*)-phenylglycinol, and then cyclized to give **1a**,**b** and **2a**,**b**, respectively.

The dicarboxylic acid **6** was prepared following the known procedure,[9] while **7** was synthesized in moderate yields by in situ carbon dioxide treatment of the 4,4′-dilithium derivative obtained by a bromine/lithium permutation with *n*-BuLi of the 4,4′-dibromo-2,2′,5,5′-tetraphenyl-3,3′-bithiophene (**10**). The latter was obtained in 60% yields starting from the hexabromo-3,3′-bithiophene, exploiting the regioselectivity of the Suzuki coupling reaction, mediated by Pd(tetrakis), in the α-positions of the thiophene rings.

The bisoxazolines with the tetramethyl scaffold were synthesized starting from dicarboxylic acid **6** that was first converted into the corresponding dichloride, using a thionyl chloride excess, and then into diamides **8a** and **8b** by reaction with (*R*)-phenylglycinol. The diastereoisomeric diamides were easily separated by column chromatography and cyclized to the corresponding bisoxazolines **1a** and **1b** by reaction with the Burgess reagent in THF solution (Scheme 4).

We couldn't apply the same synthetic scheme to the preparation of bisoxazolines **2a,b** based on the tetraphenyl scaffold, since the diamides **9a** and **9b** were obtained in very low yields and their cyclization with the Burgess reagent gave very scarce results. In fact, when the reaction was carried out at room temperature, only the monocyclized products were obtained, while at higher temperatures only **9a** was converted into the corresponding bis(oxazoline) **2a**.

In order to improve the yields in the formation of the amide bond, we performed the reaction with the (*R*)-phenylglicinol directly on the dicarboxylic acid **7**, using HOAt and HATU as coupling reagents, in the presence of DIPEA as a base and, after chromatographic separation, we were able to obtain both the diastereoisomeric diamides, although in moderate yields. Finally, we could acquire, although in unsatisfactory yields, both the bis(oxazolines) **2a** and **2b**, by subsequent ring closure of **9a** and **9b** carried out using DAST as a condensing reagent.

Chiroptical Determination of the Absolute Configuration of Bis(oxazolines) 1 and 2

Superimposed VCD (top panels) and IR (lower panels) spectra of **1a** and **1b** and of **2a** and **2b**, respectively, are reported in Figure 1. Considering that **1a** and **1b,** on the one hand, and **2a** and **2b** on the other, are diastereoisomers, differences in the IR spectra could be expected in principle. To a large extent, this does not happen and the spectra of the diastereoisomeric pairs are almost superimposable. Instead, the VCD spectra of **1a** and **1b** are mirror images to a large extent and, analogously, those of **2a** and **2b** are almost mirror images, except for minor features. These observations led us to conclude, quite naïvely but rather cogently, that in both cases VCD relates to axial stereogenicity and appears to be an excellent means to monitor the *S* vs. *R* configuration of the stereogenic axis, as observed for planar stereogenicity in the case of the cyclophane ligand cited above.[18] However, without DFT calculations it is impossible to establish whether **1a**(**2a**) is either **1a***S*(**2a***S*) or **1a***R*(**2a***R*). This will be addressed below.

In addition, systems **1** and **2** exhibit definitely different VCD spectra for compounds having the same configuration of the stereogenic axis: this implies that the normal modes corresponding to the VCD features are quite mixed combinations of group vibrations, and one can hardly isolate the specific contribution of given moieties, like those related to the central bithiophene unit (vide infra). In the case of **1**, particularly relevant is the triplet between 1050 and 1150 cm^{-1}, consisting of three features with alternating signs (+,−,+) for **1a**; while **2a** exhibits a group of features, including a (−,+) doublet from low to high wavenumbers between 1280 and 1380 cm^{-1}. Apparently, these features are unrelated, notwithstanding the fact that the two systems **1** and **2** share the same central bithiophene unit.

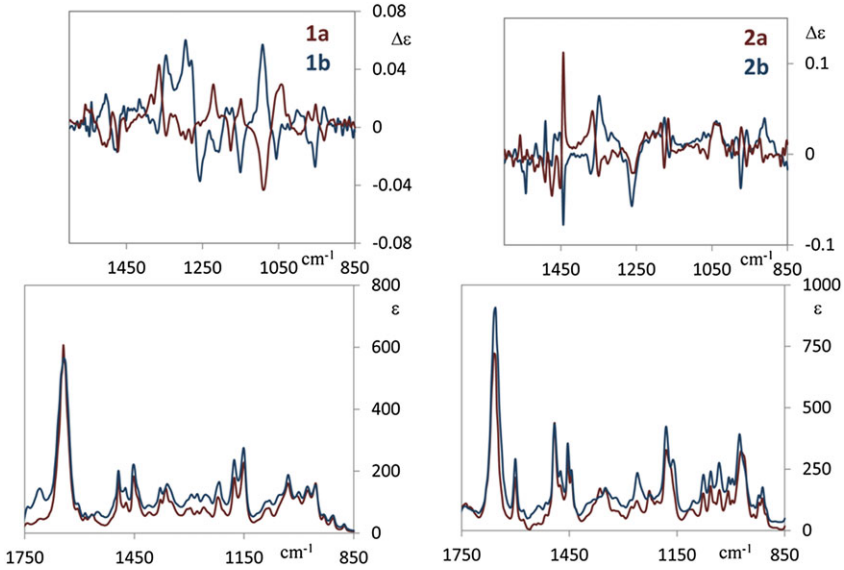

Fig. 1. Experimental VCD (top) and IR (lower) spectra of (*S*/*R*)-2,2′,5,5′-Tetramethyl-4,4′-bis[(*R*)-4,5-dihydro-4-phenyloxazol-2-yl]-3,3-bi-thiophene, **1a** and **1b** (left panels), and of (*S*/*R*)-2,2′,5,5′-tetraphenyl-4,4′-bis[(*R*)-4,5-dihydro-4-phenyloxazol-2-yl]-3,3-bithiophene, **2a** and **2b** (right panels).

In principle, the VCD spectra of diphosphane oxide **3**, characterized by the same atropisomeric core of **1a**, but devoid of any other stereogenic element, could give some help in highlighting the neat contribution of the stereogenic axis.

In this case, we found an alternating (+,−,+) triplet, though shifted to an ~1170 and 1270 cm^{-1} interval (Fig. 2); it was tempting to associate these features with those relative to the triplet observed for **1a** between ~1050 and 1150 cm^{-1}; however, this frequency difference was hard to rationalize just on a correlative basis and normal mode analysis from DFT calculations were required (vide infra).

The results of DFT calculations are summarized in Table 1, where we report for **1a**, **1b**, **2a**, **2b,** and **3** the free energy G values for the conformers within 2 kcal/mol evaluated from the most stable conformer of each one of the five systems. We also provide for each conformer the population factor, calculated as Boltzmann factors $e^{-\Delta G/RT}$ and renormalized with due account also of symmetry degeneracies (nonsymmetric conformers are counted twice).

In addition, the values for some relevant dihedral angles for **1** and **2**, whose precise definition is given in Figure SI-1 of the Supplementary Material, are reported. In short, angle θ is the inter-thiophene dihedral angle; angles ϕ measure the orientation of one oxazoline moiety with respect to the nearby thiophene; angles ω measure the puckering of oxazoline rings; and angles ψ are the dihedrals measuring the tilt of the end phenyls with respect to the closest oxazoline ring. For compound **3**, θ has the same meaning as in **1** and **2**, while ϕ and ψ are different and give a measure of the orientation of the P = O bond with respect to the closest thiophene or to the closest phenyl rings, respectively.

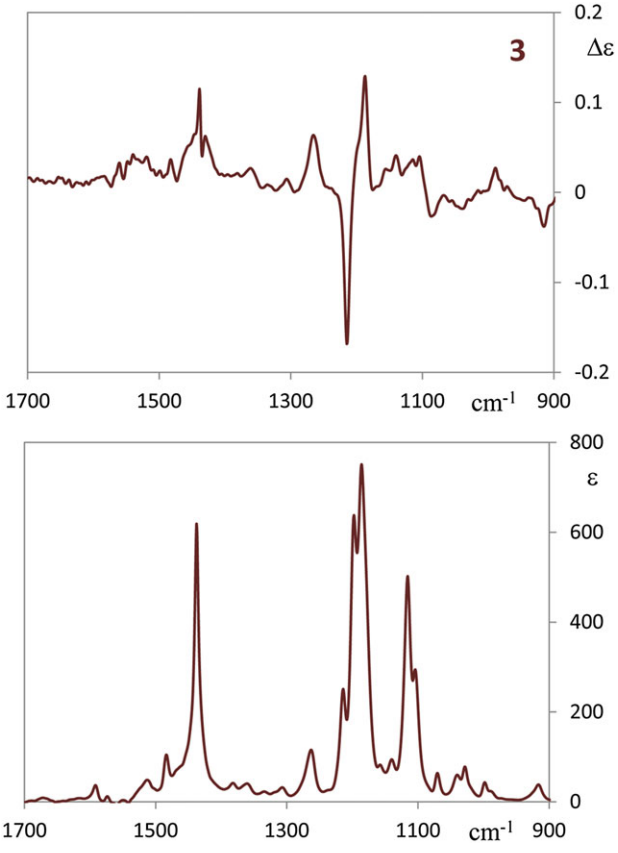

Fig. 2. Experimental VCD (top) and IR (lower) spectra of 2,2′,5,5′-Tetramethyl-4,4′-bis-(diphenyl-phosphino)-3,3′-bithiophene oxide (***3***.

The data reported in Table 1 show that the most populated conformers of 1 have θ values ca. from ±90° to ±80°, minus for a*R* and plus for a*S* axial configuration respectively (coincident with *M* and *P*, in another notation), the sign being evidently plus for **1a** and minus for **1b**, while for compounds **2** θ values range between ±75° and ±65°; this difference may be due to a combination of several factors, like different steric congestion at the bithiophene core, extended aromaticity, and π–π stacking of the phenyl substituent groups. It is interesting to note that phosphane oxide **3** has a θ value similar to that observed for **1a**.

The puckering of the oxazoline ring, as measured by the ω values, is small in all cases. The most populated conformers of **1** exhibit ϕ angle values such that the relative orientation of the N=C bond of the oxazolines with respect to the CC bond opposite to the S heteroatom of the nearby thiophene is (*anti, syn*) for **1a** and (*anti, anti*) for **1b** (within 30° from perfect *anti* and *syn* arrangement). Most of the other conformers exhibit similar ϕ values, and the (*syn, syn*) conformers are scarcely populated.

For both diastereoisomers of compound **2** we observed a prevalence of *gauche* conformers and ϕ angle values ca. ±60° and ±120° were noticed. Values for ψ are mostly small, indicating a small tilt of the end phenyl rings with respect to thiophene.

DFT calculated VCD spectra match excellently experimental VCD spectra for all investigated compounds (see Figs. 3 and 4). The comparison of experimental and calculated VCD spectra allows us to unambiguously make the following assignment of absolute configuration: **1a**↔**1**a*S*, **1b**↔**1**a*R*, **2a**↔**2**a*S*, **2b**↔**2**a*R,* **3**↔**3**a*S*. The corresponding IR absorption spectra are quite well predicted by DFT calculations (Figs. SI-2 and SI-3, respectively), even for the intense features around 1650 cm^{-1}, assigned to the stretching of the oxazoline ring bonds.

The success of the calculations may be attributable to the C_2-symmetry of the molecule; as observed in several cases.[14,27] In particular, even in the presence of many conformers, each one providing VCD features of possibly different sign, symmetry still may help, since vibrational features are either of A or B symmetry species or are duplicated for conformers without C_2-symmetry.[14]

The presence of several conformers requires discussing some apparently diagnostic features of axial or central stereogenicity such as the triplet (+,−,+) for **1a** and (−,+,−) for **1b** between 1050 and 1150 cm^{-1}. The DFT calculations for the most populated conformer of the two molecules allowed us to appreciate that the normal modes responsible for the three features are generated in the central bithiophene units (see Fig. 5).

It is reassuring to notice (Fig. SI-4) that the normal modes associated to this VCD triplet are found for all six major *aR*-conformers and four *aS*-conformers with the same signs, even if with slightly different intensities. A triplet feature quite similar to that noticed for **1a** was observed for **3** at higher wavenumbers (more than 100 cm^{-1} difference!): the change in frequency from **1** to **3** is due to the replacement of the oxazoline units with the diphenylphosphane group. This fact significantly alters the frequency position of the normal modes, without changing their aspect and VCD manifestation (see Fig. 5). This is illustrated in Table SI-1, where the frequencies, dipole and rotational strengths, g factors, and normal mode description is provided for the

TABLE 1. Conformational Analysis for 1a and 1b, for 2a and 2b, and for 3

CONF	ΔG	% pop	Symm %pop	θ	φ_1	φ_2	ω_1	ω_2	ψ_1	ψ_2
1-*aR*1	0.00	30.5	21.8	−82.6	160.2	160.2	−18.2	−18.2	38.8	38.8
1-*aR*2	0.04	28.3	40.6	−82.6	137.3	−37.9	−13.7	−14.8	10.8	33.9
1-*aR*3	0.11	25.1	18.0	−92.3	−32.9	−32.9	−15.7	−15.7	33.7	33.7
1-*aR*4	0.87	7.0	10.1	−77.4	23.6	164.1	−11.5	−15.3	42.7	36.4
1-*aR*5	1.10	4.7	3.4	−85.7	132.8	132.8	−15.4	−15.4	17.4	17.4
1-*aR*6	1.28	3.5	5.1	−85.9	−154.9	157.7	4.2	−15.5	11.9	34.1
1-*aS*1	0.00	44.0	57.3	92.2	29.0	151.9	−12.1	−16.8	41.6	41.0
1-*aS*2	0.41	22.2	14.4	90.0	161.3	161.3	−15.7	−15.7	39.0	39.0
1-*aS*3	0.74	12.5	16.3	81.3	−150.2	8.4	4.1	14.7	9.4	35.7
1-*aS*4	0.93	9.2	12.0	67.0	−146.2	−146.2	12.1	12.1	2.7	2.7
2-*aR*1	0.00	48.1	31.6	−71.8	−52.5	−52.5	−16.3	−16.3	40.8	40.8
2-*aR*2	0.36	26.3	34.6	−71.4	−46.9	124.7	−16.3	−18.8	40.8	15.3
2-*aR*3	0.53	19.7	25.9	−69.4	−51.0	137.1	−16.5	−19.8	40.8	−98.3
2-*aR*4	1.23	6.0	7.9	−72.2	−39.4	51.0	−15.4	4.8	39.1	19.8
2-*aS*1	0.00	49.9	38.7	63.6	−124.5	−124.5	−8.7	−8.7	20.8	20.8
2-*aS*2	0.61	17.8	27.6	73.8	51.2	97.1	−13.7	−14.7	40.3	24.1
2-*aS*3	0.92	10.6	16.4	72.1	−102.9	53.3	−10.9	−10.2	33.6	−1.2
2-*aS*4	1.01	9.1	14.1	69.3	61.8	−118.7	−16.6	−10.8	41.0	24.1
2-*aS*5	1.27	5.9	1.8	72.4	−62.0	46.5	−14.8	−15.4	39.5	42.9
2-*aS*6	1.50	4.0	0.6	75.1	59.8	59.8	−7.9	−7.9	3.5	3.5
2-*aS*7	1.71	2.8	0.8	75.7	100.8	49.6	−13.9	−8.7	29.6	9.7
3-*aS*1	0.00	100.0		86.3	−19.5	−19.5	−27.0	−65.9		

The free-energy values are calculated from the free-energy value of the lowest energy conformer. Population factors provided in the 3rd column are given on the basis of $e^{-\Delta G/RT}$; in the 4th column they are corrected to account for symmetry degeneracy (when needed). The relevant geometrical parameters related to internal twist of the thiophenes (θ), the orientations of oxazoline units with respect to thiophenes (φ_i, *i* = 1,2), the puckering of the oxazoline units (ω_i,i = 1,2) and the orientation of the end phenyl moieties (ψ_i, i = 1,2) are defined in the text and in Figure SI-1.

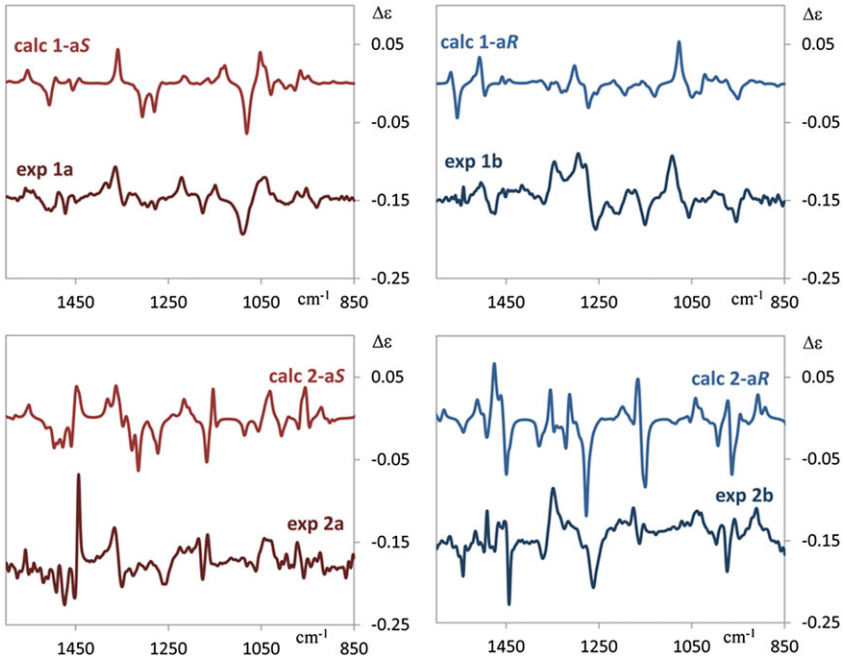

Fig. 3. Comparison of experimental and calculated VCD spectra of (*S/R*)-2,2′,5,5′-Tetramethyl-4,4′-bis[(*R*)-4,5-dihydro-4-phenyloxazol-2-yl]-3,3-bithiophene, **1a** and **1b** (top panels), and of (*S/R*)-2,2′,5,5′-tetraphenyl-4,4′-bis[(*R*)-4,5-dihydro-4-phenyloxazol-2-yl]-3,3-bithiophene, **2a** and **2b** (lower panels). Calculated VCD spectra are multiplied by a factor of 3.

dominant conformer of **1**a*R*, **1**a*S* and for the single conformer of **3**. The modes responsible for the triplet are a combination of thiophene-CC-stretchings, CH_3-deformations with some participation of adjacent groups; the latter fact is important in explaining the shift in frequency in going from **1** to **3**.

The substitution of methyl with phenyl groups has thus a dramatic impact on the three normal modes that contain large

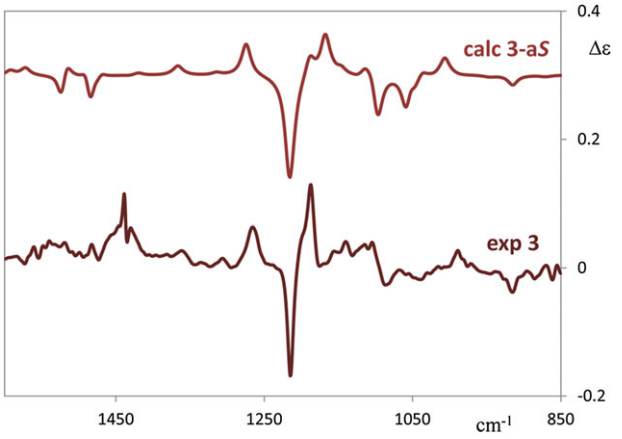

Fig. 4. Comparison of experimental and calculated VCD spectra of 2,2′,5,5′-Tetramethyl-4,4′-bis-(diphenylphosphino)-3,3′-bithiophene oxide (**3**). Calculated VCD spectrum is multiplied by a factor of 3.

amounts of CH_3-bendings and the (+,−,+)/(−,+,−) triplet was not observed any more. Indeed, the phenyl ring substitutions tend to greatly perturb the thiophene modes.

DFT calculations are in excellent agreement with the experimental data and the features of the stereogenic axis are dominating in the spectra. Once more, most of the calculated VCD features are independent of the conformer, as one may appreciate by looking at Figure SI-5 for **2a** and **2b**.

The features relative to the stereogenic centers, associated with C*H bending vibrations, are distinguishable around 1250 cm^{-1}, where a negative feature is predicted for all four bis(oxazolines) **1a**, **1b**, **2a,** and **2b**. This region had already been indicated as diagnostic for central C*H bending vibration in several cases.[18,27,28] Once more, DFT calculated normal modes demonstrate the correctness of this picture and, interestingly, this is true for all 10 major conformers of both **1** and **2** (see Figs. 3 and 4; and Figs. SI-4 and SI-5).

A further investigation was performed through ECD spectroscopy that appeared less interesting than VCD spectroscopy in the case of compounds **1**.

In fact, the ECD spectra of **1a** and **1b** are quite weak and show very little differences that are hard to reconcile with opposite axial stereogenicity. Also, DFT calculations for **1a** and **1b** do not provide mirror-image ECD spectra, while they predict experimental data excellently (Fig. SI-6). ECD spectra of bis(oxazolines) **2** are stronger and they are almost opposite for **2a** and **2b**, supporting the conclusions of opposite axial chirality drawn on the basis of VCD. Interestingly, the ECD spectrum of **3** is reminiscent of the ECD spectrum of **2a**, even though it is bathochromically shifted by ~10 nm.

The last set of chiroptical data we have taken into account are the OR values or ORD trends: the latter functions for **1** are in good correspondence with the findings based on ECD. Indeed, on the basis of the Kramers-Kronig (KK) relationship,[29–31] we expected and we observed positive values for OR in **1a** and **1b** (smaller for **1a**, vide infra) (Fig. SI-8), since the lowest-energy transition in the ECD spectrum is positive and weak for both the diastereoisomers (see Fig. 6).

Also in the case of the diphosphane oxide **3,** the OR data were, as expected, negative, namely ca. –65 at 589 nm.[32] Moreover, the two diastereoisomers of bis(oxazoline) **1**, characterized by opposite configuration of the stereogenic axis, exhibited OR with the same sign, while **1a** and **3**, which exhibit the same configuration of the atropisomeric core, show opposite sign.

On the basis of these results it is clear that it isn't possible to associate the observed OR sign with the configuration of the stereogenic axis.

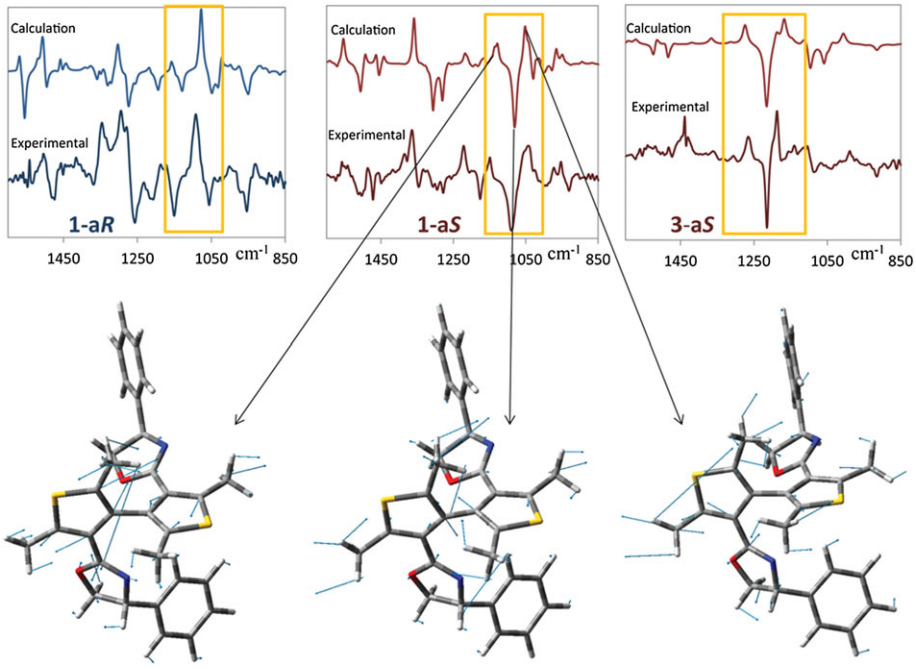

Fig. 5. The assignment of the VCD triplet of bands diagnostic of axial chirality for **1a** and **1b** (*S/R*)-2,2′,5,5′-Tetramethyl-4,4′-bis[(*R*)-4,5-dihydro-4-phenyloxazol-2-yl]-3,3-bithiophene 2,2′,5,5′-Tetramethyl-4,4′-bis-(diphenyl-phosphino)-3,3′-bithiophene oxide (**3**). The computational algorithm and graphics of Gaussian09[23] was employed.

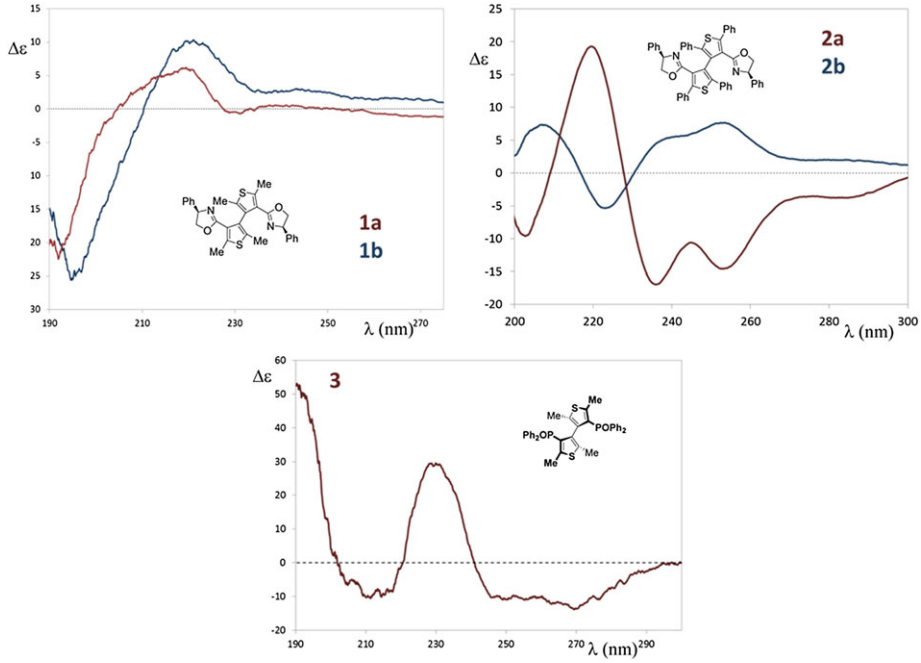

Fig. 6. Experimental ECD spectra of **1a** and **1b**, **2a** and **2b**, **3.**

CONCLUSIONS

The configurational and conformational properties of several variants of chiral C_2-symmetric phenyl bisoxazoline ligands based on the 3,3′-bithiophene atropisomeric scaffold, **1** and **2**, differing for the substituents (methyl or phenyl) on the thiophene rings, were investigated as a premise for the possible application of their transition metal complexes as catalysts in stereoselective synthesis.

In particular, comparing the effects of the presence of methyl and phenyl groups on the bithiophene scaffold, it is interesting to note that, in the former case, a rather relevant increase in the dihedral angle θ, from 65–75° to 80–90°, is produced. This should strongly influence the bite angle in the corresponding metal complexes and, as a consequence, their catalytic activity and stereoselection ability.

The analysis was carried out by employing three chiroptical techniques (VCD, ECD, and ORD), interpreting the spectra in the IR and UV ranges through DFT calculations. The analysis of the bis(oxazoline) ligands was completed by comparing the results with the data recorded for the C_2 symmetric diphosphane **3**, sharing the same bithiophene scaffold as **1**.

VCD spectra were found of primary importance in the determination of the absolute configuration of all the compounds and in monitoring their conformational properties. As regards the absolute configuration assignment, we established that **1a**(**2a**)↔a*S* **1b**(**2b**)↔a*R*. We notice that, for tetramethyl substituted compounds **1**, VCD was much more informative than ECD. Indeed, characteristic VCD signals directly related to the configuration of the stereogenic axis have been identified in all molecules **1–3**, and have been explained in terms of normal modes involving the bithiophene central unit of the molecules, even if a major influence by substituents on the normal modes is recorded. Instead ECD spectra for **1a** and **1b** have the same signs, as well as the ORD curves; both tetramethyl derivatives are dextrorotatory and thus the sign of OR does not have a discriminating value for configuration, and neither does ECD. Indeed, it can be noticed that stereogenic oxazolines carbons drive overall chirality such that ECD and ORD are not able to discriminate diastereomers **1a** and **1b**. On the contrary in **2a** and **2b** and in **3** the phenyl groups, which are responsible of ECD signals, are more directly related to axial stereogenicity.

As a general comment on the usefulness of VCD versus ECD, we may state that VCD spectra contain distinct signals related to both axial and to central stereogenicity for systems **1** and **2**, while ECD cannot discriminate the two types of chiralities.

ACKNOWLEDGMENTS

We thank CARIPLO foundation for funding the research program. We thank also CILEA and CINECA for computational facilities e progetto LISA. The first two authors contributed equally to this work.

SUPPORTING INFORMATION

Additional supporting information may be found in the online version of this article at the publisher's web-site.

LITERATURE CITED

1. Benincori T, Brenna E, Sannicolò F, Trimarco L, Antognazza P, Cesarotti E. Heteroaromatic diphosphines as chiral ligands. WO9601831 A1; Date: 25/01/1996.
2. Benincori T, Brenna E, Sannicolò F, Trimarco L, Antognazza P, Cesarotti E. (Diphenylphosphino)-biheteroaryls: the first example of a new class of chiral atropisomeric chelating diphosphine ligands for transition metal catalysed stereoselective reactions. J Chem Soc Chem Commun 1995; 685.
3. Benincori T, Brenna E, Sannicolò F, Trimarco L, Antognazza P, Cesarotti E, Demartin F, Pilati T. New class of chiral diphosphine ligands for highly efficient transition metal-catalyzed stereoselective reactions: the bis (diphenylphosphino)five-membered biheteroaryls. J Org Chem 1996; 61: 6244.

4. Benincori T, Piccolo O, Rizzo S, Sannicolò F. 3,3′-Bis (diphenylphosphino)-1,1′-disubstituted-2,2′-biindoles: easily accessible, electron-rich, chiral diphosphine ligands for homogeneous enantioselective hydrogenation of oxoesters. J Org Chem 2000; 65: 8340.
5. Celentano G, Benincori T, Radaelli S, Sada M, Sannicolò F. Effects of the electronic properties of chiral chelating diphosphines in stereoselective Diels-Alder cycloaddition reactions promoted by their transition metals complexes. J Organomet Chem 2002; 643–644: 424.
6. Tietze LF, Thede K, Sannicolò F. Regio- and enantio- selective Heck reactions of aryl and alkenyl triflates with the new chiral ligand (R)-BITIANP. J Chem Soc Chem Commun 1999; 1811.
7. Tietze LF, Thede K, Schimpf R, Sannicolò F. Enantioselective Synthesis of Tetrahydroquinolines and Benzazepines by Silane Heck Reactions with the Chiral Ligands (+)-TMBPT and (R)-BITIANP. J Chem Soc Chem Commun 2000; 583–584.
8. Benincori T, Cesarotti E, Piccolo O, Sannicolò F. 2,2′,5,5′-Tetramethyl-4,4′-bis(diphenylphosphino)-3,3′-bithiophene: A new, very efficient, easily accessible, chiral biheteroaromatic ligand for homogeneous stereoselective catalysis. J Org Chem 2000; 65: 2043.
9. Benaglia M, Benincori T, Mussini P, Pilati T, Rizzo S, Sannicolò F. Steric and electronic tuning of chiral bis(oxazoline) ligands with 3,3′-bithiophene backbone. J Org Chem 2005; 70: 7488.
10. Nafie LA. Vibrational optical activity, principles and applications. John Wiley & Sons: Hoboken, NJ; 2011.
11. Keiderling TA. In: Nakanishi K, Berova N, Woody RW, editors. Circular dichroism: principles and applications. Wiley-VCH Publishers: New York; 2000 . p 621–666.Chapter 22
12. Polavarapu PL, Zhao C. Vibrational circular dichroism: a new spectroscopic tool for biomolecular structural determination. Fresenius J Anal Chem 2000; 366: 727–734.
13. Taniguchi T, Monde K. The exciton chirality method in vibrational circular dichroism. J Am Chem Soc 2012; 134: 3695–3698.
14. Passarello M, Abbate S, Longhi G, Lepri S, Ruzziconi R, Nicu VP. Importance of C*-H based modes and large amplitude motion effects in vibrational circular dichroism spectra: the case of the chiral adduct of dimethyl fumarate and anthracene. J Phys Chem A 2014; 118: 4339–4350.
15. Buffeteau T, Ducasse L, Brizard A, Huc I, Oda R. Density Functional Theory calculations of vibrational absorption and circular dichroism spectra of dimethyl-L-tartrate. J Phys Chem 2004; 108: 4080–4091.
16. Su CN, Keiderling TA. Conformation of dimethyl tartrate in solution. Vibrational circular dichroism results. J Am Chem Soc 1980; 102: 511–515.
17. Abbate S, Castiglione F, Lebon F, Longhi G, Longo A, Mele A, Panzeri W, Ruggirello A, Turco LV. Spectroscopic and structural investigation of the confinement of D and L dimethyl tartrate in lecithin reverse micelles. J Phys Chem B 2009; 113: 3024–3033.
18. Abbate S, Burgi LF, Castiglioni E, Lebon F, Longhi G, Toscano E, Caccamese S. Assessment of configurational and conformational properties of naringenin by vibrational circular dichroism. Chirality 2009; 21: 436–441.
19. Polavarapu PL, Jeirath N, Kurtàn T, Pescitelli G, Krohn K. Determination of the absolute configurations at stereogenic centers in the presence of axial chirality. Chirality 2009; 21: E202–E207.
20. Polavarapu PL, Petrovic AG, Vick SE, Wulff WD, Ren H, Ding Z, Staples RJ. Absolute configuration of 3,3′-diphenyl-[2,2′-binaphthalene]-1,1′-diol revisited. J Org Chem 2009; 74: 5451–5457.
21. He Y, Wang B, Dukor RK, Nafie LA. Determination of absolute configuration of chiral molecules using vibrational optical activity: a review. Appl Spectrosc 2011; 65: 699–723.
22. Abbate S, Ciogli A, Fioravanti S, Gasparrini F, Longhi G, Pellacani L, Rizzato E, Spinelli D, Tardella PA. Solving the puzzling absolute configuration determination of a flexible molecule by vibrational and electronic circular dichroism spectroscopies and DFT calculations: the case study of a chiral 2,2′-dinitro-2,2′-biaziridine. Eur J Org Chem 2010; 6193–6199.
23. Gaussian 09, Revision A.02, Frisch MJ, Trucks GW, SchlegelHB, ScuseriaGE, Robb MA, Cheeseman JR, Scalmani G, Barone V, Mennucci B, Petersson GA, Nakatsuji H, Caricato M, X L, Hratchain HP, Izmaylov AF, Bloino J, Zheng G, Sonnenberg JL, Hada M, Ehara M, Toyota K, Fukuda R, Hasegawa J, Ishida M, Nakajima T, Honda Y, Kitao O, Nakai H, Vreven T, Montgomery JA Jr, Peralta JE, Ogliaro F, Bearpark M, Heyd JJ, Brothers E, Kudin KN, Staroverov VN, Kobayashi R, Normand J, Raghavachari K, Rendell A, Burant JC, Iyengar SS, Tomasi J, Cossi M, Rega N, Millam JM, Klene M, Knox JE, Cross JB, Bakken V, Adamo C, Jaramillo J, Gomperts R, Stratmann RE, Yazyev O, Austin AJ, Cammi R, Pomelli C, Ochterski JW, Martin RL, Morokuma K, Zakrzewski VG, Voth GA, Salvador P, Dannenberg S, Dapprich S, Daniels AD, Farkas Ö, Foresman JB, Ortiz JV, Cioslowski J, Fox DJ. Gaussian. Gaussian, Inc.: Wallingford, CT; 2009.
24. Stephens PJ. The theory of vibrational circular dichroism. J Phys Chem 1985; 89: 748–750.
25. Bruhn T, Schaumlöffel A, Hemberger Y, Bringmann G. SpecDis: quantifying the comparison of calculated and experimental electronic circular dichroism spectra. Chirality 2013; 25: 243–249.
26. Yin Y, Sun G, Zhang H, Zhu H, Wu F. Chin. Enantioselective Calchogeno-Baylis-Hillman reaction of amylaldehyde with MKV and acrylates catalyzed by chiral thiepin-$TiCl_4$ complex. J Chem 2014; 32: 365.
27. Abbate S, Mazzeo G, Meneghini S, Longhi G, Boiadjiev SE, Lightner DA. Bicamphor: a prototypic molecular system to investigate vibrational excitons. J Phys Chem A 2015; 119: 4261–4267.
28. Abbate S, Burgi LF, Castiglioni E, Lebon F, Longhi G, Toscano E, Caccamese S. Assessment of configurational and conformational properties of naringenin by vibrational circular dichroism. Chirality 2009; 21: 436–441.
29. Moscowitz A. Theoretical aspects of optical activity. part one: small molecules. Adv Chem Phys 1962, IV, 67–112. Prigogine I, editor. New York: Interscience.
30. Polavarapu PL, Petrovic AG, Zhang P. Kramers-Kronig transformation of experimental electronic circular dichroism: application to the analysis of optical rotatory dispersion in dimethyl-L-tartrate. Chirality 2006; 18: 723–732.
31. Giorgio E, Viglione RG, Zanasi R, Rosini C. Ab initio of optical rotatory dispersion (ORD) curves: a simple an reliable approach to the assignment of the molecular absolute configuration. J Am Chem Soc 2004; 126: 12968–12976.
32. Rossi S; Benaglia M, Genoni A, Benincori T, Celentano G. Biheteroaromatic diphosphine oxides-catalyzed stereoselective direct aldol reactions. Tetrahedron 2011;67:158–166.